

Noise and the Measurement Process for a Circular Josephson Array Qubit

Joachim Sjöstrand and Anders Karlhede

Department of Physics, Stockholm University, Albanova University Center, SE-10691 Stockholm, Sweden

(Dated: November 1, 2018)

We discuss a charge qubit consisting of a circular array of Josephson junctions. The two-level system we consider couples the two charge states through a higher order tunneling process thus making it possible to achieve a long relaxation time. Using the spin-boson Hamiltonian, we estimate decoherence due to ohmic as well as $1/f$ noise. We simulate the quantum mechanical measurement process by studying the density matrix of the qubit and a capacitively coupled single-electron transistor that measures the charge.

I. INTRODUCTION

In recent years much effort has been spent on the search for quantum two-level systems, qubits, that can be coherently controlled long enough for a sequence of controlled unitary operations to be performed on them. The ultimate goal is to build a quantum computer out of these qubits. Proposals for qubits based on a variety of physical systems exist, each with its pros and cons. Here we consider solid state charge qubits based on Josephson junctions (JJ) arrays. These have the advantage of being relatively easy to manipulate and the prospects for large scale manufacturing are comparatively good. However, they suffer from severe decoherence effects. The single Cooper-pair box (SCB) is the simplest proposal for a charge based JJ qubit.¹ For the SCB, superposition of charge states was observed by Bouchiat *et al.*³ and coherent evolution was demonstrated by Nakamura *et al.*²

A generalisation of the SCB, which we call the circular array (CA), was introduced by Schöllmann *et al.*⁴ This circuit consists of an array of tunable JJs in a circular geometry. The CA is similar to the SCB and many results can be taken over *mutatis mutandis*. The main difference is that the two charge states of the qubit are coupled through a higher order tunneling process. Turning the coupling off then allows the tunneling rate to be made very small – leading to slow relaxation, and a long time to perform the measurement. This is the key element of the quantum sample and hold (QUASH) measurement strategy.⁴

In this article we perform a more detailed study of the circular array. In particular, we consider the effect of voltage fluctuations in the circuit (ohmic noise) as well as $1/f$ noise, believed to be caused by background charge fluctuations, and calculate the relaxation and dephasing times for these types of noise – extending the previous treatment.⁴ We also study the measurement of the qubit’s charge by a single-electron transistor (SET) coupled capacitively to the CA. This is done by numerically determining the time development of the density matrix following the treatment of Makhlin *et al.*⁶ for the SCB.

II. THE CIRCULAR ARRAY

The circular array consists of two arrays with N identical JJs each – these arrays are connected in series and separated by a capacitor C_0 , thus forming a circular geometry. Each JJ, which is a small SQUID, has capacitance C_J and a Josephson energy $E_J = E_J(\Phi(t))$ which can be tuned by altering the magnetic flux Φ through the SQUID loop. The lead connecting the two arrays is grounded to allow charge to tunnel in and out of the circuit. There are $2N$ small islands, $i = 1, 2, \dots, 2N$, each characterized by the number of excess Cooper pairs n_i and the phase of the superconducting order parameter ϕ_i ; these are quantum mechanically conjugate variables: $[\phi_i, n_j] = i\delta_{ij}$. Each island charge is externally controlled by a gate voltage $V_i(t)$, applied via a small capacitor C_g . Fig. 1 shows the circular array together with the SET that measures the charge on one of the islands next to C_0 .

A qubit should have two states separated by a large gap, δE , from higher energy states and be weakly coupled to the environment to avoid rapid decoherence. The CA fulfills this if $C_0 \sim C_J \gg C_g$. The energy scales present in the system is the charging energy for a Cooper pair $E_C \equiv (2e)^2/2C_J \sim \delta E$, the Josephson energy E_J , the superconducting gap Δ and the temperature $k_B T$. In order to avoid quasiparticles in the system at low temperatures, the qubit is constructed so that Δ is the largest energy in the problem. Furthermore, we choose the qubit to be in the charge regime $E_C \gg E_J$, and impose $E_C \gg k_B T$ to avoid thermal excitation of higher energy charge states, thus:

$$\Delta \gg E_C \gg E_J, k_B T . \quad (1)$$

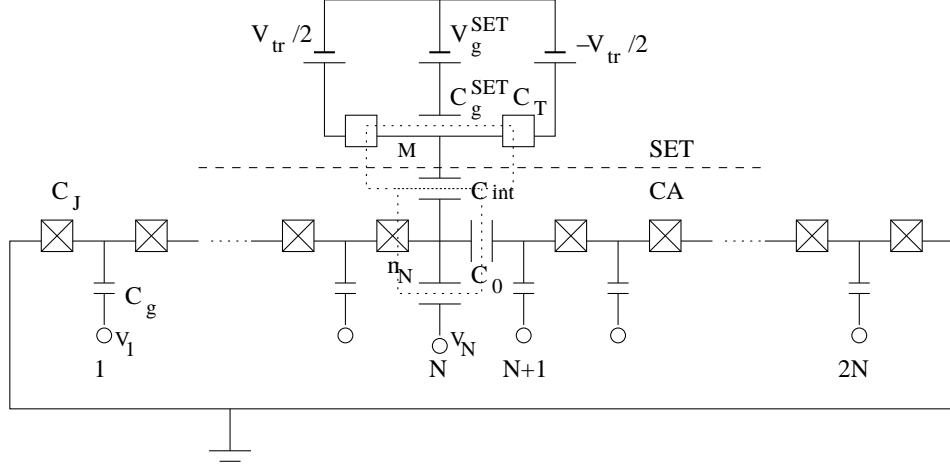


FIG. 1: The circular array with a SET connected to island N . The box symbols (without cross) stand for normal junctions. Island N on the CA and the island of the SET is marked with dotted boxes.

The Hamiltonian of the CA is

$$H = H_C + H_J = \frac{1}{2} \sum_{i,j=1}^{2N} Q_i C_{ij}^{-1} Q_j - E_J \sum_{\langle ij \rangle} \cos(\phi_i - \phi_j) , \quad (2)$$

where $Q_i = 2e(n_i - n_{g,i})$ is the effective charge on island i – here $n_{g,i} = C_g V_i / 2e$ is the gate charge on the island. C_{ij} is the capacitance matrix – its nonzero elements are: $C_{N,N} = C_{N+1,N+1} = C_0 + C_J + C_g$, $C_{i,i} = 2C_J + C_g$, $C_{N+1,N} = C_{N,N+1} = -C_0$ and $C_{i+1,i} = C_{i,i+1} = -C_J$, where $i \neq N, N+1$. The matrix is symmetric and $C_{ij} = C_{2N+1-i, 2N+1-j}$; the inverse matrix C^{-1} has the same symmetries. The sum over the Josephson terms in (2) is taken over all pairs of islands connected by tunnel junctions.

Since we are studying a charge qubit it is convenient to write the Hamiltonian in the charge basis $|\mathbf{n}\rangle = |n_1 n_2 \dots n_{2N}\rangle$. The charging energy term simply becomes $H_C = E_C C_J \sum_{\mathbf{n}} (\mathbf{n} - \mathbf{n}_g)^t C^{-1} (\mathbf{n} - \mathbf{n}_g) |\mathbf{n}\rangle \langle \mathbf{n}|$ where $\mathbf{n}_g = (n_{g,1}, n_{g,2}, \dots, n_{g,2N})$, and using that $|n_i\rangle = \int_0^{2\pi} d\phi_i e^{-in_i \phi_i} |\phi_i\rangle$, which holds since n_i and ϕ_i are conjugate, the Josephson term becomes

$$H_J = -\frac{E_J}{2} \sum_{\mathbf{n}, \langle ij \rangle} \prod_{k \neq i,j} |n_k\rangle \left(|n_i+1\rangle |n_j-1\rangle + |n_i-1\rangle |n_j+1\rangle \right) \langle \mathbf{n}| \quad (3)$$

and the total Hamiltonian is $H = H_C(\mathbf{V}) + H_J(\Phi)$, where we have indicated the dependence on the external control parameters $\mathbf{V} = (V_1, V_2, \dots, V_{2N})$ and Φ .

The two-level system – *ie* the qubit – we consider consists of states $|\uparrow\rangle, |\downarrow\rangle$ with one excess Cooper pair on either of the islands $N, N+1$ neighbouring C_0 : $|\uparrow\rangle \equiv |0 \dots 10 \dots 0\rangle$ and $|\downarrow\rangle \equiv |0 \dots 01 \dots 0\rangle$, where the ones are for island N and $N+1$ respectively. For $E_J = 0$ these two states are degenerate if $n_{g,N} = n_{g,N+1} = \frac{1}{2}$ and $n_{g,i} = 0$ for $i \neq N, N+1$. If, in addition, $C_0 \sim C_J \gg C_g$, then the energy gap to higher charge states is $\delta E \sim E_C$. Restricting ourselves to a finite charge space, the Hamiltonian H can be diagonalised numerically. In Fig. 2 we show the energy spectrum for the $N = 2$ CA as a function of $n_{g,2}$. The other parameters are $n_{g,3} = 1/2$, $C_0 = C_J = 100C_g$, $E_J = 0.2E_C$ and $-2 \leq n_i \leq 2$ (this restriction gives a negligible error). For $n_{g,2} \approx 1/2$, the two lowest energy levels (which are linear combinations of the states $|\uparrow\rangle, |\downarrow\rangle$ with an excess Cooper pair on island N or $N+1$ respectively) form a two-level system with a large gap to the higher energy states.

We conclude that when $E_C \gg E_J$, $C_0 \sim C_J \gg C_g$ and $\mathbf{n}_g \approx (0, \dots, \frac{1}{2}, \frac{1}{2}, \dots, 0)$, it is a good approximation to restrict the Hilbert space of the Hamiltonian in Eq. (2) to the states $|\uparrow\rangle$ and $|\downarrow\rangle$ defined above. We write the Hamiltonian of this two-level system in spin-1/2 notation

$$H_{ctrl}(t) = -\frac{1}{2} B_z(\delta V(t)) \sigma_z - \frac{1}{2} B_x(\Phi(t)) \sigma_x , \quad (4)$$

where σ_i are the Pauli matrices in the basis $(|\uparrow\rangle, |\downarrow\rangle)$. This Hamiltonian controls the qubit – unitary operations can be performed on the qubit by tuning B_z and B_x via the external parameters $\delta V = V_{N+1} - V_N$ and Φ . Writing

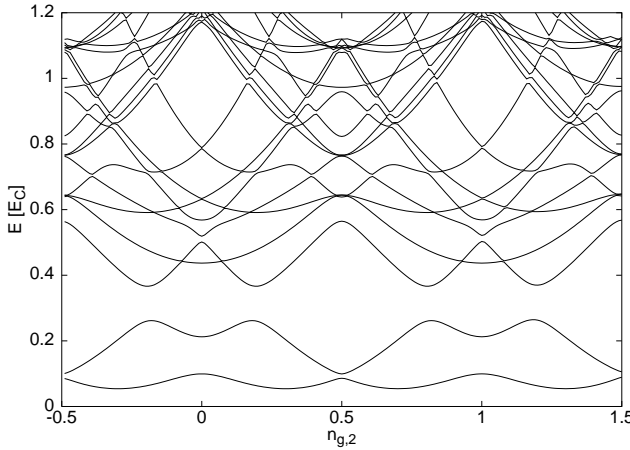


FIG. 2: The energy levels for the $N = 2$ CA as functions of $n_{g,2}$. The other parameters are $E_J = 0.2E_C$, $n_{g,3} = 0.5$ and $C_J = C_0 = 100C_g$. (Charge states with $-2 \leq n_i \leq 2$ are included in the diagonalization.)

$\mathbf{n}_g = (0, \dots, \frac{1+\delta n_g}{2}, \frac{1-\delta n_g}{2}, \dots, 0)$ where $\delta n_g = C_g \delta V / 2e$, we find $B_z = \langle \downarrow | H_C | \downarrow \rangle - \langle \uparrow | H_C | \uparrow \rangle = 2A_N E_C \delta n_g$, where $A_N = C_J (C_{NN}^{-1} - C_{N,N+1}^{-1})$. A_N can be calculated numerically for given capacitance matrix, however, we can also perform an expansion in C_g/C_0 which is valid as long as N is not too large. Using Cramer's rule for the elements in C^{-1} , we express A_N in terms of cofactors and expand. Assuming, for simplicity, $C_J = C_0$, this gives

$$B_z = \frac{2N}{2N+1} \left[1 - \frac{C_g}{C_0} \frac{N+1}{6} + \mathcal{O}((C_g/C_0)^2) \right] \times E_C \delta n_g . \quad (5)$$

(For $N = 2$ and to leading order in C_g , this reproduces a previous result.⁴) B_x gives the cotunneling rate of a Cooper pair from island N to $N+1$ via the $2N$ junctions and its leading contribution is obtained by $(2N)^{th}$ order perturbation theory, hence $B_x \sim (E_J/E_C)^{2N}$. The exact numerical factor is not very illuminating – it can however be determined for not too large N . For the $N = 2$ CA, with parameters as in Fig. 2, we have $B_z \approx \frac{4}{5} \left[1 - \frac{1}{2} \frac{C_g}{C_0} \right] E_C \delta n_g = 0.796 E_C \delta n_g$ and $B_x = \frac{125}{12} (E_J/E_C)^4 E_C = 0.0167 E_C^4$. (A numerical diagonalisation gives $B_z = 0.7960 E_C \delta n_g$ and $B_x = 0.0132 E_C$ – in reasonable agreement with the expansions taking into account that the ignored terms are of order $\mathcal{O}((C_g/C_0)^2) \sim 10^{-4}$ and $\mathcal{O}((E_J/E_C)^6) \sim 10^{-4}$ respectively.)

Diagonalizing (4) gives the eigenvalues $\pm \frac{1}{2} \Delta E$ where $\Delta E = \sqrt{B_x^2 + B_z^2}$, with corresponding eigenvectors $|+\rangle = \cos \frac{\theta}{2} | \uparrow \rangle + \sin \frac{\theta}{2} | \downarrow \rangle$, and $|-\rangle = -\sin \frac{\theta}{2} | \uparrow \rangle + \cos \frac{\theta}{2} | \downarrow \rangle$, where $\theta = \arctan(B_x/B_z)$. If τ denotes the Pauli matrices in the energy eigenbasis, then H_{ctrl} can be written in the compact form

$$H_{ctrl} = -\frac{1}{2} \Delta E \tau_z . \quad (6)$$

III. ELECTROMAGNETIC NOISE

The practical usefulness of a circuit like the CA as a qubit is ultimately limited by the coupling to external degrees of freedom. These lead to decoherence of the qubit state and hence loss of quantum information to the environment. The generic behaviour of the evolution of the qubit depends on the strength of the coupling and one identifies two regimes: The “Hamiltonian-dominated”, where the coupling to the environment is weak enough for the time evolution of the qubit to be governed by the qubit Hamiltonian H_{ctrl} , and the “environment-dominated”, where the coupling to the environment is so strong that it determines the dynamics of the qubit. In this article we consider only the Hamiltonian-dominated regime. Note, however, that even if the coupling to the environment is weak under normal operation of the qubit, it becomes environment-dominated if $H_{ctrl} \approx 0$, which may happen during the qubit manipulations.

In the Hamiltonian-dominated regime the evolution of the qubit is conveniently described in the energy eigenbasis ($|-\rangle$, $|+\rangle$). The interaction with the environment leads to a decay of the off-diagonal elements in the qubit's density matrix with a characteristic time τ_φ , the dephasing time,

$$\langle \tau_\pm(t) \rangle = \langle \tau_\pm(0) \rangle e^{\mp i \Delta E t} e^{-t/\tau_\varphi} ; \quad (7)$$

whereas the diagonal elements of the density matrix decay to their thermal equilibrium values with a characteristic time τ_{relax} , the relaxation time,

$$\langle \tau_z(t) \rangle = \tau_z(\infty) + (\tau_z(0) - \tau_z(\infty))e^{-t/\tau_{relax}} , \quad (8)$$

where the thermal equilibrium value is $\tau_z(\infty) = \tanh(\Delta E/2k_B T)$.

A Josephson junction charge qubit is sensitive to various electromagnetic fluctuations in the circuit; we follow standard practice and model these with the “spin-boson” model⁷ with an Ohmic spectrum. In addition to the noise caused by these fluctuations one observes $1/f$ noise, which is believed to be due to background charge fluctuations in the substrate. Following Shnirman *et al.*⁸ we model this phenomenologically using again the spin-boson model but now with a $1/f$ -spectrum.

The spin-boson model describing the qubit interacting with the environment has one independent bath for each island in the CA:

$$H_{SB} = H_{ctrl} + \sigma_z \sum_{i=1}^{2N} X_i + \sum_{i=1}^{2N} H_B^i . \quad (9)$$

Here, H_{ctrl} is the qubit Hamiltonian (4), $H_B^i = \sum_{a,i} \left(\frac{p_{ai}^2}{2m_{ai}} + \frac{m_{ai}\omega_{ai}x_{ai}^2}{2} \right)$ is a bath of harmonic oscillators with coordinates x_{ai} , momenta p_{ai} , masses m_{ai} and frequencies ω_{ai} . The baths lead to voltage fluctuations $X_i \equiv \sum_a C_{ai}x_{ai}$ coupling to σ_z . (C_{ai} is the strength of the coupling between the qubit and the a'th oscillator in bath i .)

The effect of the environment is completely characterized by a spectral function, which for the spin-boson model in Eq. (9) has the form

$$J(\omega) = \frac{\pi}{2} \sum_{a,i} \frac{C_{ai}^2}{m_{ai}\omega_{ai}} \delta(\omega - \omega_{ai}) = \frac{\pi}{2} \sum_i \alpha_s^i \hbar \omega_{00}^{1-s} \omega^s \Theta(\omega_c - \omega) . \quad (10)$$

To obtain the second equality one assumes that $J(\omega)$ can be written as a power of ω up to some cut-off frequency ω_c which is assumed to be large compared to all other frequencies in the problem. The parameter s reflects the qualitative nature of the environment, and $\alpha_s \equiv \sum_i \alpha_s^i$ is a dimensionless measure of the strength of the coupling. To maintain α_s dimensionless for all s , an additional frequency scale ω_{00} enters for $s \neq 1$.

We model the voltage fluctuations δV_i on island i by adding an impedance $Z_i(\omega)$ in series with V_i , see, *eg*, Ingold and Nazarov⁹ or Makhlin *et al.*⁵ This impedance then has Johnson-Nyquist fluctuations δV_i between its terminals that in the spin-boson formalism correspond to the spectral function $J_i(\omega) = \omega \text{Re} [Z_{it}(\omega)]$, where $Z_{it}(\omega)$ is the total impedance between the terminals of Z_i . From Fig. 1 one finds $Z_{it}(\omega) = [i\omega C_{\Sigma i} + Z_i^{-1}(\omega)]^{-1}$ where $C_{\Sigma i}^{-1} = C_g^{-1} + (s_i C_0)^{-1}$, with $s_i = i^{-1} + (2N+1-i)^{-1}$ (assuming $C_J = C_0 \gg C_g$). Following standard practice, we assume that the noise is purely resistive, $Z_i(\omega) = R_i$, and if furthermore $R_i \ll 1/\omega C_{\Sigma i}$ (which holds for realistic R_i and C_g since $C_{\Sigma,i} < C_g$), we obtain $J_i(\omega) = \omega R_i$, which is linear in ω and hence corresponds to $s = 1$ in Eq. (10). Using this we can obtain the total spectral function $J(\omega)$ for the circuit. From Eq. (9) we identify $X = -\frac{1}{2}\delta B_z$, where $\delta B_z = [\langle \downarrow | H_C | \downarrow \rangle - \langle \uparrow | H_C | \uparrow \rangle] \Big|_{n_i^g = \frac{C_g}{2e} \delta V_i}$. Simplifying this expression yields $X = -e \frac{C_g}{C_J} \sum_{i=1}^{2N} A_i \delta V_i$, with $A_i \equiv C_J \left(C_{N+1,i}^{-1} - C_{N,i}^{-1} \right)$. The fluctuations δV_i are expressed in the oscillator coordinates, $\delta V_i = \sum_a b_{ia} x_{ia}$, with the spectral function in the form of Eq. (10), $J_i(\omega) = \frac{\pi}{2} \sum_a \frac{b_{ia}^2}{m_{ia}\omega_{ia}} \delta(\omega - \omega_{ia}) = \omega R_i$. This gives $X = -e \frac{C_g}{C_J} \sum_{i=1}^{2N} A_i \sum_a b_{ia} x_{ia}$ and hence, $J(\omega) = \omega \sum_i \left[-e \frac{C_g}{C_J} A_i \right]^2 R_i$. Comparing this to Eq. (10), with $s = 1$, we find

$$\alpha_1 = 4 \sum_i A_i^2 \cdot \frac{R_i}{R_K} \left(\frac{C_g}{C_J} \right)^2 , \quad (11)$$

where $R_K = h/e^2 = 25.8 \text{ k}\Omega$ is the quantum of resistance. Assuming the islands to be nearly identical, it is reasonable that R_i are approximately the same for all islands. Setting $R_i = R$, $i = 1, \dots, 2N$, we are left with the factor $\sum_i A_i^2$, which we can calculate numerically for given capacitance matrix or as an expansion in C_g/C_0 . The expansion is analogous to the one for B_z in Eq. (5) – assuming for simplicity $C_J = C_0$ we obtain

$$\alpha_1 = \frac{4N(N+1)}{3(2N+1)} \left[1 - \frac{2C_g}{15C_0} (N^2 + N + 3) + \mathcal{O}((C_g/C_0)^2) \right] \times \frac{R}{R_K} \left(\frac{C_g}{C_0} \right)^2 . \quad (12)$$

(For $N = 2$ and to leading order in C_g , Eq. (12) gives $\alpha_1 = \frac{8}{5} \frac{R}{R_K} \left(\frac{C_g}{C_J} \right)^2$ as derived previously.⁴) Fig. 3 shows α_1 as a function of N for different C_g/C_0 . The numerical result is shown as crosses, and the expansion to order $(C_g/C_0)^3$ as squares. For $C_g/C_0 = 10^{-2}$ and 10^{-3} , the expansion agrees very well with the numerical result (at least when

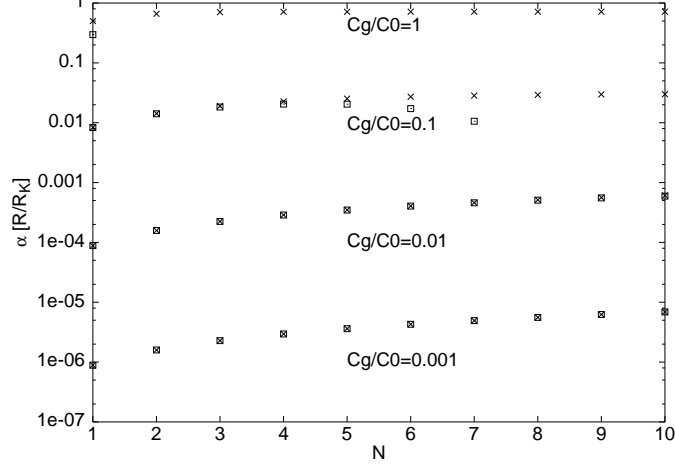


FIG. 3: α_1 as a function of N for different C_g/C_0 . The numerical result is shown as crosses and the analytic expansion as squares. α_1 is given in units of R/R_K and the scale on the y -axis is logarithmic; $R_i = R$ for all islands, and $C_J = C_0$.

$N \leq 10$). For $C_g/C_0 = 0.1$ and 1, the expansion becomes negative at $N \geq 8$ and $N \geq 2$ respectively. Therefore no squares are seen in this region. In a typical circuit we may have $R \sim 50 \Omega$, yielding $R/R_K \sim 10^{-3}$. For $C_g \ll C_0$, $\alpha_1 \ll 1$ for all realistic N .

The characteristic times τ_{relax} and τ_φ can be calculated within the spin-boson model using perturbation theory or path integral methods.¹⁰ For $s = 1$ they are

$$\Gamma_{relax} \equiv \tau_{relax}^{-1} = \frac{1}{\hbar^2} \sin^2 \theta \cdot S_X(\Delta E/\hbar) = \pi \alpha_1 \frac{\Delta E}{\hbar} \coth \frac{\Delta E}{2k_B T} \sin^2 \theta , \quad (13)$$

$$\Gamma_\varphi \equiv \tau_\varphi^{-1} = \frac{1}{2} \Gamma_{relax} + \frac{1}{\hbar^2} \cdot S_X(0) = \frac{1}{2} \Gamma_{relax} + \pi \alpha_1 \theta \frac{2k_B T}{\hbar} \cos^2 \theta , \quad (14)$$

where

$$S_X(\omega) \equiv \langle [X(t), X(t')]_+ \rangle_\omega = 2\hbar J(\omega) \coth \frac{\hbar\omega}{2k_B T} \quad (15)$$

is the Fourier transform of the symmetrized correlation function at thermal equilibrium. These results can be applied to the CA simply by substituting α_1 from Eq. (11). One defines the pure dephasing rate Γ_φ^* , as $\Gamma_\varphi = \frac{1}{2} \Gamma_{relax} + \cos^2 \theta \Gamma_\varphi^*$. The Hamiltonian-dominated regime is realized when $\Delta E \gg \hbar \Gamma_\varphi^*$ (at least for $s = 0, 1$ ¹²). For ohmic damping, $\Gamma_\varphi^* = 2\pi \alpha_1 k_B T / \hbar$, and the condition becomes $\Delta E \gg \alpha_1 k_B T$.

Noise with a power spectrum proportional to the inverse of the frequency is observed in many physical systems. This $1/f$ noise is seen also in JJ circuits¹¹, where it is believed to be caused by background charge fluctuations.¹³ Here we follow Shnirman *et al.*⁸ and model this noise with the spin-boson model. For $s = 0$ and $\omega \ll k_B T / \hbar$, (15) gives the wanted power spectrum: $S_X(\omega) = E_{1/f}^2 / \omega$ with $E_{1/f}^2 = 2\pi \hbar \alpha_0 \omega_{00} k_B T$ (here T is an adjustable parameter). Sub-ohmic environments (*ie* those for which $0 \leq s < 1$) have not been much studied as it was believed that they rapidly localized the system in one of the σ_z -eigenstates for any strength of the damping. However, it has been realized that this is true only for large damping, whereas for weak damping the system behaves coherently¹⁴. The times τ_{relax} and τ_φ have been calculated for $1/f$ noise for the single bath spin-boson model in the Hamiltonian-dominated regime⁸. The relaxation rate is

$$\Gamma_{relax} = \frac{E_{1/f}^2}{\hbar \Delta E} \sin^2 \theta . \quad (16)$$

The dephasing rates are only known for $\theta = 0, \pi/2$; they are

$$\Gamma_\varphi = \frac{E_{1/f}}{\hbar} \sqrt{\frac{1}{\pi} \ln \frac{E_{1/f}}{\hbar \omega_{ir}}} \quad \text{for } \theta = 0 \quad (17)$$

and

$$\Gamma_\varphi = \frac{E_{1/f}^2}{\hbar\Delta E} \frac{1}{2\pi} \ln \frac{E_{1/f}^2}{\hbar\omega_{ir}\Delta E} \quad \text{for } \theta = \pi/2, \quad (18)$$

both with logarithmic accuracy in $E_{1/f}$ ⁸. Here, ω_{ir} is an infrared cut-off frequency which can be experimentally determined. To determine the times we need to determine $E_{1/f}$.¹⁶

IV. THE QUANTUM MEASUREMENT OF CHARGE

The state of the qubit is inferred by performing a quantum measurement of the charge using a SET coupled capacitively to island N of the circular array, see Fig. 1. We simulate this quantum measurement by studying the time development of the density matrix describing the CA and the SET – we follow closely Makhlin *et al.*,⁶ where the corresponding problem is treated for the SCB.

The SET is a circuit with one normal island surrounded by two junctions connected to normal electrodes and a capacitor C_g^{SET} , see Fig. 1. During manipulations of the qubit, no current flows through the SET – the SET is turned off – this is achieved by setting the transport voltage to zero, $V_{tr} = 0$, and tuning the gate voltage V_g^{SET} away from a degeneracy point so that the Coulomb blockade suppresses the tunneling through the SET. When the manipulations of the qubit are done and one wants to read out the result, then the Coulomb blockade is turned off by tuning the gate voltage to a degeneracy point and a transport voltage is turned on leading to a tunneling current through the SET. This current depends on the state of the qubit through the charge on the capacitor C_{int} . This leads to a measurement of the charge of the qubit.

The density matrix for the CA and the SET can be written as $\hat{\rho} \equiv \hat{\rho}(i, i', M, M', m, m')(t)$ after one has traced out the microscopic degrees of freedom in the left and right electrodes and in the island of the SET. Here, i labels the state of the qubit, M is the number of (excess) electrons on the island in the SET and m is the number of electrons that have tunneled through the SET. It is possible to derive a master equation for $\hat{\rho}$ as an expansion in the SET tunneling terms.¹⁵ For low temperature and small V_{tr} , only transitions between two adjacent charge states of the SET need to be taken into account (these states are assumed to be $M = 0, 1$ below). If one furthermore assumes that the tunneling is instantaneous then one obtains a set of simple equations for the diagonal matrix elements $\hat{\rho}_M^{ij}(m, t) \equiv \hat{\rho}(i, j; M, M; m, m)(t)$. In terms of the Fourier transformed quantity $\hat{\rho}_M^{ij}(k, t) = \sum_m e^{-ikm} \hat{\rho}_M^{ij}(m, t)$, the final form is a system of eight coupled differential equations (for each k)

$$\hbar \frac{d}{dt} \begin{pmatrix} \hat{\rho}_0 \\ \hat{\rho}_1 \end{pmatrix} + \begin{pmatrix} i[H_{ctrl}, \hat{\rho}_0] \\ i[H_{ctrl} + \delta H_{int}, \hat{\rho}_1] \end{pmatrix} = \begin{pmatrix} -\check{\Gamma}_L & e^{-ik}\check{\Gamma}_R \\ \check{\Gamma}_L & -\check{\Gamma}_R \end{pmatrix} \begin{pmatrix} \hat{\rho}_0 \\ \hat{\rho}_1 \end{pmatrix}, \quad (19)$$

where $\hat{\rho}_M$ is short for the 2×2 matrix $\hat{\rho}_M^{ij}(k, t)$. H_{ctrl} is the qubit Hamiltonian with a renormalised capacitance matrix ($C_{N,N} \rightarrow C_{N,N} + C_{int}$) due to the presence of the SET, $\delta H_{int} = E_{int}\sigma_z$ is the coupling energy where E_{int} is determined by the capacitances. The tunneling rates $\Gamma_{L/R}$ are

$$\begin{aligned} \check{\Gamma}_L \hat{\rho}_0 &\equiv \Gamma_L \hat{\rho}_0 + \pi\alpha_L [\delta H_{int}, \hat{\rho}_0]_+, \\ \check{\Gamma}_R \hat{\rho}_1 &\equiv \Gamma_R \hat{\rho}_1 - \pi\alpha_R [\delta H_{int}, \hat{\rho}_1]_+, \end{aligned} \quad (20)$$

where $\alpha_{L/R}$ and $\Gamma_{L/R}$ is the tunneling conductance and the tunneling rate for the left/right junction of the SET.

We want to study the current through the SET as a function of time – this is obtained from

$$P(m, t) \equiv \sum_{i, M} \hat{\rho}(i, i, M, M, m, m)(t), \quad (21)$$

which can be interpreted as the probability that m electrons have tunneled through the SET during time t . To compute $P(m, t)$, we solve the differential equation (19) with suitable initial conditions. We assume that the qubit and the SET are disentangled initially, $\hat{\rho}(t=0) = \hat{\rho}_0^{qb} \otimes \hat{\rho}_0^{SET}$, and that the qubit is prepared in some state $|\psi\rangle = \alpha |\uparrow\rangle + \beta |\downarrow\rangle$, $\hat{\rho}_0^{qb} = |\psi\rangle\langle\psi|$. At time $t=0$, no electrons have tunneled through the SET, thus $P(m, 0) = \delta_{m,0}$ and $P(k, 0) = 1$ for the Fourier transform. From the definition (21), we find $P(k, 0) = \text{Tr}(\hat{\rho}_0) + \text{Tr}(\hat{\rho}_1)$ and we may choose $(\hat{\rho}_0, \hat{\rho}_1)|_{t=0} = (\mathbf{0}, \hat{\rho}_0^{qb})$.

To calculate $P(m, t)$ for the $N = 2$ CA we need values for the parameters E_{int} , α_L , α_R , Γ_L and Γ_R for the SET, and B_z and B_x for the qubit. We choose $C_g = C_{int} = C_g^{SET} = \frac{1}{3}C_T = \frac{1}{100}C_J = \frac{1}{100}C_0 = 0.032$ fF, $\alpha_L = \alpha_R = 0.03$, $\Gamma_L = 30$ μ eV and $\Gamma_R = 100$ μ eV (the qualitative result will not be too sensitive to this choice). Hence $E_C = 100$ μ eV,

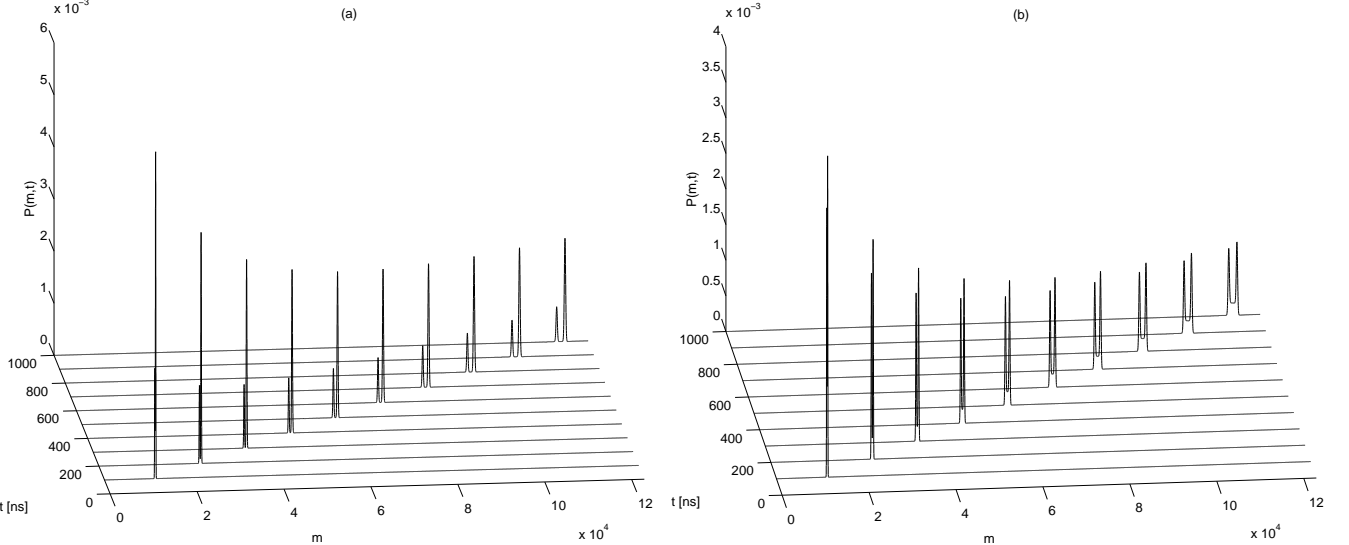


FIG. 4: $P(m, t)$ as a function of m for ten different times t . In (a), $B_x = 0$, $B_z = 9.0 \mu\text{eV}$ and $|\alpha|^2 = 0.75$, whereas in (b), $B_x = 1.3 \mu\text{eV}$, $B_z = 15 \mu\text{eV}$ and $|\alpha|^2 = 0.50$.

$E_{int} = 6.1 \mu\text{eV}$ and $B_z = 80\delta n_g \mu\text{eV}$. At the start of the measurement B_x is turned off, $B_x \simeq 0$. B_z is kept close to the degeneracy point, although $B_z \neq 0$ to avoid the environment-dominated regime. Fig. 4 shows examples of $P(m, t)$. In (a) a measurement in the off-state, $B_x = 0$, is shown, the other parameters are $B_z = 9.0 \mu\text{eV}$ (corresponding to $\delta n_g = 0.11$) and $|\alpha|^2 = 0.75$. For comparison, Fig. 4(b) shows a measurement where B_x is on; the parameters are in this case $B_x = 1.3 \mu\text{eV}$ (which is the maximum value of B_x assuming $E_J^{max} = 0.2E_C$), $B_z = 15 \mu\text{eV}$ (corresponding to $\delta n_g = 0.19$) and $|\alpha|^2 = 0.50$. We see that after a while, P develops a two peak structure. This is interpreted as follows. At a given time, the total current is a superposition of two different currents flowing in the SET, with weights given by the amplitudes, α and β , of the charge states in the qubit state. For increasing t , the peaks move towards higher m values since more electrons have tunneled through the SET. During this process, the peaks widen, their magnitude decreases and the distance (in m) between the peaks increases. The ratio between the two peak values are 2.96 in Fig. 4(a) and 1.10 – 1.20 (the value decreases with time) in Fig. 4(b) to be compared to the ratios $|\alpha|^2/|\beta|^2 = 3$ and 1 respectively. Fig. 4(a) corresponds to our proposed measurement situation – the off-state – and we see that here the peaks are well separated after a while and the ratio of their peak values stay close to $|\alpha|^2/|\beta|^2$ for a very long time. Thus allowing for a slow accurate measurement of the charge. In Fig. 4(b) on the other hand, the peaks are less well separated and the ratio agrees less well with $|\alpha|^2/|\beta|^2$. Eventually the valley between the peaks will fill out and one broad peak forms due to mixing between the charge states – a plateau indicating this process is clearly seen in (b). To perform a measurement of the charge, the peaks must have moved apart to become well separated and not yet started to merge due to mixing. This gives a window in time for measuring the charge – in the off-state in Fig. 4(a) this window is very large – the lower bound is $\tau_{meas} \sim 500 \text{ ns}$. The upper bound is not seen, however, we expect it to be considerably larger.

V. DISCUSSION

We here estimate the decoherence times for the circular array. To be specific we assume $C_0 = C_J = 100C_g$, $E_C \simeq 5E_J^{max} \simeq 100 \mu\text{eV}$ and $T \simeq 40 \text{ mK} = 3 \mu\text{eV}$ and, initially $N = 2$ – higher N are commented on below.

Calculations are performed by tuning $H_{ctrl}(t)$ in time. During this process the SET is off, and we are close to the degeneracy point. Assuming $|\delta n_g| \lesssim 0.2$, then $|B_z| \lesssim 0.16E_C \simeq 16 \mu\text{eV}$ – in addition we have $|B_x| \lesssim 0.013E_C = 1.3 \mu\text{eV}$. There is also a lower bound on ΔE , since the system is assumed to be in the Hamiltonian-dominated regime. The typical time per operation of the qubit is $\tau_{op} \simeq \hbar/\Delta E \sim 10 \text{ ps}$ assuming $\Delta E \simeq 10 \mu\text{eV}$.

For the ohmic noise, we use $R \simeq 50 \Omega$, which gives $\alpha_1 \simeq 3 \cdot 10^{-7}$. Assuming $\Delta E \lesssim 16 \mu\text{eV}$ one finds $\tau_\varphi \sim 100 \mu\text{s}$ and $\tau_{relax} \gtrsim 100 \mu\text{s}$. The Hamiltonian regime is realised when $\Delta E \gg \alpha_1 k_B T \approx 10^{-12} \text{ eV}$.

For $1/f$ noise, τ_φ is only known for $\theta = 0$ and $\theta = \pi/2$. We use these two cases to estimate τ_φ , assuming that this gives the correct order of magnitude for general θ . Nakamura *et al.*¹¹ measured the factor $\alpha_{1/f}^{SCB} = (E_{1/f}^{SCB})^2/E_C^2$

for the SCB and obtained $\alpha_{1/f}^{SCB} \sim 10^{-6}$. If the $1/f$ -noise is caused by background charge fluctuations then it is reasonable to assume that for the CA $\alpha_{1/f} \simeq 2N\alpha_{1/f}^{SCB}$, since the CA has $2N$ islands instead of the single island in the SCB. This gives $E_{1/f}^2 = 2\pi\hbar\alpha_0\omega_{00}k_B T \simeq 2NE_C^2\alpha_{1/f}^{SCB}$ and, for the parameters above, we find $E_{1/f}^2 \simeq 4 \cdot 10^{-6}E_C^2$. From Nakamura *et al.*¹¹ we also take $\omega_{ir} \simeq 310$ Hz. For $\theta = 0$ we find $\tau_{relax} \rightarrow \infty$ and $\tau_\varphi \sim 1$ ns if $B_z < 16$ μ eV and for $\theta = \pi/2$, we find $\tau_{relax} \sim 10$ ns and $\tau_\varphi \sim 5$ ns if $B_x < 1.3$ μ eV. This shows that the Hamiltonian-dominated regime is realised if $\Delta E \gg 0.5$ μ eV.

After the calculations, the SET is turned on and the measurement is started by tuning B_x to 0. The relaxation is now very slow: $\tau_{relax} \rightarrow \infty$ when $\theta \rightarrow 0$ for both ohmic and $1/f$ noise. This gives ample time to measure $|\alpha|^2$ without using an ultra-fast detector, *c.f.* Fig. 4. The dephasing is very rapid, thus the quantum state of the qubit is destroyed in a short time but it is still possible to measure the charge. This is good enough as a read-out measurement but not as part of an error correction protocol.

For higher N , the ohmic decoherence times will decrease somewhat, due to an increase in α_1 . The same is true for $1/f$ noise, since $E_{1/f} \sim \sqrt{N}$.

We conclude that it is the $1/f$ noise that limits the operation of the CA as a qubit – it leads to the decoherence time $\tau_{decoh} \sim 1$ ns. The decoherence due to ohmic noise is much slower. Hence, in practice, the ohmic noise seems to be of little concern. If the typical time for a quantum operation is $\tau_{op} \sim 10$ ps, then the $1/f$ noise restricts one to $N_{op} \sim 100$ operations, assuming B_x and B_z are restricted to values that realise the Hamiltonian-dominated regime. This is a severe restriction and once again underscores that $1/f$ noise is a serious problem for Josephson junction charge qubits. One possible solution to this might be the echo-technique demonstrated by Nakamura *et al.*¹¹.

Acknowledgments

We wish to thank Peter Ågren, Jochen Walter, Silvia Corlevi, Janik Kailasvuori and Hans Hansson for useful discussions and Sergei Isakov for his computer skills. Anders Karlhede was supported by the Swedish Science Research Council.

¹ A. Shnirman, G. Schön and Z. Hermon, *Phys. Rev. Lett.* **79**, 2371 (1997).
² Y. Nakamura, Y. A. Pashkin and J. S. Tsai, *Nature* **398**, 786 (1999).
³ V. Bouchiat, D. Vion, P. Joyez, D. Esteve and M. H. Devoret, *Physica Scripta* vol T76, 165-170 (1998).
⁴ V. Schöllmann, P. Ågren, D. B. Haviland, T. H. Hansson and A. Karlhede, *Phys. Rev. B* **65**, 020505(R) (2002).
⁵ Y. Makhlin, G. Schön and A. Shnirman, *Nature* **386**, 305 (1999).
⁶ Y. Makhlin, G. Schön and A. Shnirman, *Rev. Mod. Phys.*, **73**, 357 (2001).
⁷ A. O. Caldeira and A. J. Leggett, *Ann. Phys. (N.Y.)* **149**, 374 (1983).
⁸ A. Shnirman, Y. Makhlin and G. Schön, cond-mat/0202518 (2002).
⁹ G.-L. Ingold and Y. Nazarov, *Single charge tunneling*, NATO ASI Series, Vol. B 294, edited by H. Grabert and M. H. Devoret (Plenum Press, New York, 1992).
¹⁰ A. J. Leggett *et al.*, *Rev. Mod. Phys.* **59**, 1 (1987).
¹¹ Y. Nakamura, Yu. A. Pashkin, T. Yamamoto and J. S. Tsai, *Phys. Rev. Lett.* **88**, 047901 (2002).
¹² U. Weiss, *Quantum dissipative systems*, World Scientific, Singapore (1992).
¹³ A. B. Zorin *et al.*, *Phys. Rev. B* **53**, 13682 (1996).
¹⁴ S. Kehrein and A. Mielke, *Phys. Lett. A* **219**, 313 (1996).
¹⁵ H. Schoeller and G. Schön, *Phys. Rev. B* **50**, 18436 (1994).
¹⁶ The relaxation rate is in fact given by Eq. (13) with $S_X(\omega) = E_{1/f}^2/\omega$, whereas Eq. (14) cannot be used for the dephasing rates since $S_X(0) \rightarrow \infty$ for $s = 0$.